Interdisciplinary Research in Medical Sciences Specialty
ISSN: 3062-4401
2026, Volume 6, Issue 1, Page No: 164-177

Available online at: www.galaxypub.co/page/journals

Galaxy Publication

Isolation of Circulating Tumor Cells from Cancer Patients Using Surface Charge–Based Nanotechnology

Luca Ferraro[1]*, Matteo Ricci[1], Giulia Moretti[2], Paolo Greco[3]

[1]Department of Liquid Biopsy and Circulating Tumor Cells, Faculty of Medicine, University of Bologna, Bologna, Italy.
[2]Department of Nanotechnology and Surface Charge Isolation, Faculty of Medicine, University of Turin, Turin, Italy.
[3]Department of Cancer Diagnostics and CTC Capture, Faculty of Medicine, Sapienza University of Rome, Rome, Italy.

***E-mail** ✉ luca.ferraro@unibo.it

Received: 21 January 2026; **Revised:** 15 April 2026; **Accepted:** 19 April 2026

ABSTRACT

Circulating tumor cells (CTCs) provide an essential foundation for core cancer research and for reliably assessing the outcomes of medical treatments. Yet, recovering CTCs from patient blood samples remains technically demanding, with the main obstacles stemming from limitations in biomarker selectivity and the overall sensitivity of isolation procedures. In an earlier investigation, we introduced an innovative detection strategy for CTCs centered on a defining biophysical property of cancer cell surfaces: a negative electrical charge controlled by glycolytic metabolism. The present work reports experimental validation of this strategy's performance in isolating CTCs from clinical blood specimens collected from patients diagnosed with solid tumors and leukemia. Results show that the technique can recover tens of thousands of living cancer cells from multiple metastatic solid tumors and leukemia cases using as little as 1 mL of blood. These isolated cells were counted via cytological imaging based on morphological traits typical of malignant cells. Our data confirm that the negatively charged surface is a consistent feature shared by both laboratory-cultured cancer cell lines and freshly obtained blood samples from individuals with cancer. Moreover, the nanomaterial-based capture platform used here outperformed earlier techniques, substantially improving the identification and preservation of CTCs for downstream confirmation and detailed study. These advances offer strong potential to refine cancer diagnostics and to better track patient responses to therapy.

Keywords: Circulating tumor cells, Leukemia, Nanomaterial-based CTC detection technology, Solid tumors

How to Cite This Article: Ferraro L, Ricci M, Moretti G, Greco P. Isolation of Circulating Tumor Cells from Cancer Patients Using Surface Charge–Based Nanotechnology. Interdiscip Res Med Sci Spec. 2026;6(1):164-77. https://doi.org/10.51847/AKPZMbf6B6

Introduction

In 1869, Ashworth first identified cancerous cells in a stained blood smear taken from a patient with cancer and examined under a microscope. Although groundbreaking, this observation attracted minimal interest for nearly 130 years and only received widespread attention in the late 1990s, once its broader implications were recognized [1, 2].

Distant metastasis in solid cancers occurs when malignant cells detach from the primary tumor and travel to remote locations within the body [3, 4]. This distant spread is possible only through the vascular circulation, where the detached cells are referred to as circulating tumor cells (CTCs) [5]. Previous research has established that a single gram of solid tumor can release as many as one million cancer cells each day [6]. While the majority of these formerly anchorage-dependent cells fail to survive the turbulent conditions of blood flow, a small proportion resists hemodynamic shear stress and immune surveillance, enabling them to initiate secondary tumors [7].

CTCs occupy a central position in the metastatic sequence. Their presence and abundance in peripheral blood indicate both the invasive potential of the primary tumor into the vasculature and the risk of establishing distant metastatic sites. Over recent years, the scientific community has increasingly appreciated the clinical utility of CTC quantification and phenotypic analysis for predicting disease progression, estimating prognosis, and informing treatment choices [8, 9]. Because CTCs appear in the bloodstream during the initial phases of invasive malignancy, they also represent promising candidates for early cancer screening [10, 11]. Leukemia, which commonly arises in the bone marrow, frequently releases abundant abnormal cells straight into the circulation [12]. Consequently, isolating leukemia cells from other blood components holds importance for disease management and for detecting minimal residual disease [13].

Owing to the extreme rarity of CTCs in blood, effective enrichment and subsequent examination are crucial for any meaningful clinical translation. However, existing capture methods suffer from notable shortcomings and poor reproducibility, resulting in unacceptably low recovery rates in both research and diagnostic settings. Most current platforms isolate only a handful to several dozen CTCs from a standard 7.5-mL blood volume [14, 15]. Such incomplete recovery can compromise clinical decision-making and prevents robust statistical analysis when cell numbers are minimal. A primary reason for these shortcomings lies in the reliance on biological features that are not truly cancer-specific [15]. Typical enrichment strategies target epithelial-specific surface proteins [16, 17], tissue-specific antigens [18], cell size [19], or surface area [20]. Unfortunately, these traits are neither universal among tumor cells nor exclusive to them, which compromises both sensitivity and specificity [21]. For example, relying on cell diameter is unreliable because certain tumor cells (such as those in small cell lung cancer) are smaller than many normal blood cells. In addition, many carcinoma cells experience epithelial-mesenchymal transition (EMT) before dissemination, further reducing the effectiveness of marker-based approaches [22, 23]. As a result of these limitations, relatively few CTC isolation technologies have achieved routine clinical adoption [24, 25].

Our 2016 research revealed that metabolically active cancer cells in culture universally display a pronounced negative surface charge, in contrast to normal blood cells and organ progenitor cells, which carry either neutral or weakly positive charges [26]. This distinctive negative charge arises from elevated lactic acid production linked to the cancer cells' altered glycolytic pathway, a phenomenon known as the "Warburg effect" [27]. These observations prompted the hypothesis that surface charge differences could serve as a reliable means to separate normal cells from malignant ones. Positively charged nanoprobes (NPs) developed in that work demonstrated selective binding to the surfaces of cancer cells regardless of histological type or anatomical origin [26]. Once bound, the labeled cancer cells could be efficiently retrieved using magnetic force, leaving behind cells without significant negative surface charge. Importantly, this approach causes minimal cellular damage, preserving the captured CTCs for advanced analyses such as molecular subtyping or ex vivo expansion. Building on these results, the present study assessed the capacity of this nanomaterial-based platform to enhance CTC recovery from blood samples of hospitalized patients presenting with different malignancies at varying clinical stages.

Materials and Methods

Reagents and materials

All starting chemicals and reagents were sourced from commercial vendors. Key materials for nanoprobe synthesis included Iron (III) chloride hydrate ($FeCl_3 \bullet 6H_2O$), tetraethyl orthosilicate (TEOS), (3-Aminopropyl) triethoxysilane (APTES), Rhodamine B isothiocyanate (RBITC), and Polyetherimide (PEI, 99%, MW = 10,000), purchased from Sigma-Aldrich. Culture media and related supplements were obtained from Gibco Corporation. Remaining solutions were prepared in deionized water (18.2 MΩ·cm; Thermo Fisher Scientific). Antibodies directed against EpCAM, CD45, and CK-19 for immunofluorescence experiments were acquired from Abcam.

Preparation of the charged NPs

Superparamagnetic nanoparticles were initially produced through a solvothermal reaction. Sodium acetate and $FeCl_3 \bullet 6H_2O$ were dissolved in ethylene glycol under constant magnetic stirring to form a uniform yellow solution, which was then placed in a Teflon-lined stainless steel autoclave and heated at 200°C for 10 h. The resulting particles underwent three washing cycles with ethanol and deionized water. In the next stage, the magnetic cores were coated with TEOS to produce negatively charged particles. Fluorescent labeling was achieved by adding APTES-RBITC and allowing the reaction to proceed for 20 h protected from light. The mixture was washed three times as described previously. Finally, positive surface charge was introduced by modifying the particles with PEI

under mild stirring combined with ultrasonication for 2 h. The completed nanoprobes were washed three additional times with deionized water.

Characterization of the charged NPs

The morphology of the charged nanoparticles was examined using a Philips Tecnai 20 transmission electron microscope. Scanning electron microscopy was performed on a JEOL SM4800 instrument. Zeta potential measurements of the magnetic nanoprobes were conducted in aqueous medium at ambient temperature with a Zetasizer Nano-ZS90 dynamic light scattering analyzer (Malvern, UK). Fluorescence microscopy images were captured with an inverted Nikon Ti-U microscope equipped with a CCD camera. Confocal imaging was carried out using a Leica TCS SPE laser scanning confocal microscope.

Cell culture

Human cell lines, including the leukemia line K562, breast cancer line MDA-MB-231, lung cancer line A549, and bladder cancer lines 5637 and J82, were obtained from ATCC. These lines were cultured in RPMI 1640 or DMEM medium containing 10% (v/v) heat-inactivated fetal bovine serum and 1% (v/v) penicillin-streptomycin. Incubation occurred at 37°C in a humidified atmosphere with 5% CO_2. Routine passaging was performed by trypsin treatment, with cells maintained under the specified conditions.

Blood sample collection

Peripheral blood was collected from healthy volunteers who provided informed consent, following approval by the institutional review board (IRB). Samples were drawn into EDTA vacutainers and handled within 24 hours of collection. For validation experiments, cultured cells from different lines were introduced into these blood specimens as spiked controls.

Capture of cancer cells from the clinical blood samples

The study included blood specimens from 20 healthy donors and 2321 cancer patients who had undergone surgery at Quanzhou First Hospital in Fujian and Tongji University Oriental Hospital in Shanghai. The patient group comprised 14 individuals with leukemia, 6 with bladder carcinoma, 386 with colon cancer, 321 with liver cancer, 265 with rectal cancer, 295 with lung cancer, 153 with gastric cancer, 117 with pancreatic cancer, 127 with esophageal cancer, 138 with breast cancer, 79 with osteosarcoma, 46 with bile duct cancer, 19 with cervical cancer, 23 with duodenal cancer, 18 with gallbladder cancer, and 314 with other cancer types. All clinical samples were obtained after informed consent under an approved IRB protocol. For leukemia cases, 10 μL blood aliquots were prepared in triplicate and diluted in 2 mL PBS (200-fold dilution) to limit interference from plasma proteins. For solid tumor patients, 1 mL whole blood aliquots were processed in triplicate using discontinuous Percoll density gradient centrifugation to isolate the mononuclear cell fraction. These cells were resuspended in 2 mL PBS and incubated with the nanoprobes under rotation for 10 min. The tubes were then positioned on a magnetic rack for 10 min to immobilize NP-bound cells against the vessel wall. After discarding the supernatant, the tubes were washed twice with PBS while on the rack. Finally, the tubes were removed from the magnetic field and the enriched cells were carefully resuspended in 100 μL PBS.

Enumeration of the captured cancer cells

Following magnetic separation, the recovered cells were resuspended and transferred onto glass slides via cytocentrifugation prior to Diff-Quik staining. Every cell displaying the morphological traits characteristic of malignancy, as outlined earlier, was identified and tallied across the entire slide. Final counts were corrected for the dilution factor and reported as cancer cell numbers per milliliter of whole blood. Samples processed at the beginning of the study were confirmed by experienced pathologists holding appropriate licensure. Later samples were assessed and quantified by laboratory technologists who had completed comprehensive training under pathologist supervision..

Immunofluorescence staining

Captured cells intended for immunofluorescence analysis were first resuspended in PBS and cytocentrifuged onto coated glass slides at 500 rpm for 3 minutes. After air-drying for 5 minutes, the preparations were fixed in 4% paraformaldehyde for 12 minutes. Slides were rinsed twice with PBS and then treated with 5% Triton X-100 in PBS for 20 minutes to permeabilize the cells. Subsequent washes included one step with 0.2% Tween in PBS and

two steps with PBS. Blocking was performed using 10% bovine serum albumin for 1 hour at ambient temperature, followed by two PBS rinses. Primary antibodies specific for CD45, CK19, and EpCAM were prepared at a 1:200 dilution in 0.5% BSA and applied overnight at 4°C. On the following day, slides underwent washing with 5% BSA containing 0.2% Tween in PBS, then with PBS. Secondary antibodies (anti-mouse-FITC, anti-rabbit-AF561, or anti-rabbit-AF647) were diluted 1:200 in 0.5% BSA and incubated with the slides for 30 minutes at room temperature. After three PBS washes, nuclear counterstaining was carried out with 10 mM DAPI for 5 minutes, and the slides were coverslipped using ProLong Gold Antifade mounting medium.

Results and Discussion

Controls and quality control

Prior to processing clinical blood specimens from cancer patients, the performance characteristics of the nanoprobes (NPs) and the overall tumor cell capture efficiency were thoroughly validated **(Figure 1)**. **Figure 1a** illustrates the full workflow of the charge-based cancer cell isolation process. Cancer cells derived from several established cell lines were suspended either in phosphate-buffered saline (PBS) or in normal whole blood. Recovery rates obtained from PBS primarily evaluate the inherent functionality of the NPs, while those from whole blood provide a more complete assessment that accounts for both NP performance and procedural handling. In cases involving solid tumors, 1 mL of whole blood was typically analyzed. For leukemia samples, however, only 10 µL of whole blood diluted in PBS was used, given the possibility of markedly elevated tumor cell numbers. Mononuclear cells were then separated from the blood or PBS suspensions using discontinuous precooled gradient centrifugation. Charged NPs were subsequently introduced and incubated briefly with the cell suspension. A magnet was applied to the tube exterior to attract and immobilize all NP-bound cells against the vessel wall. These cells underwent several PBS washes to eliminate nonspecific adherence. Equal quantities of the enriched cells were then deposited onto glass slides by cytocentrifugation, fixed, and stained with Diff-Quik to enable cytomorphological examination and manual enumeration.

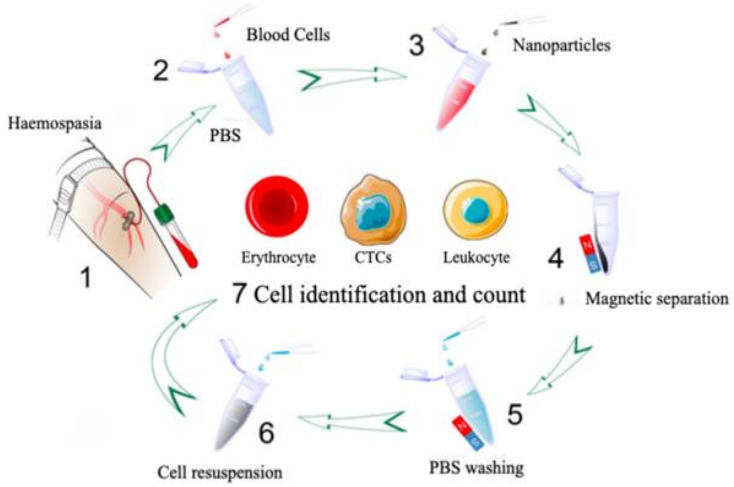

a)

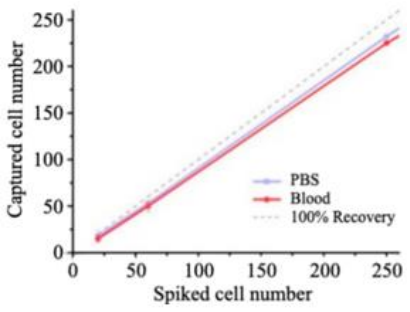

b)

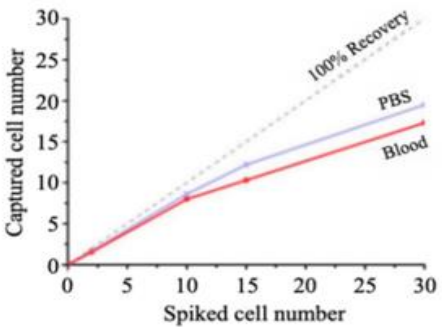

c)

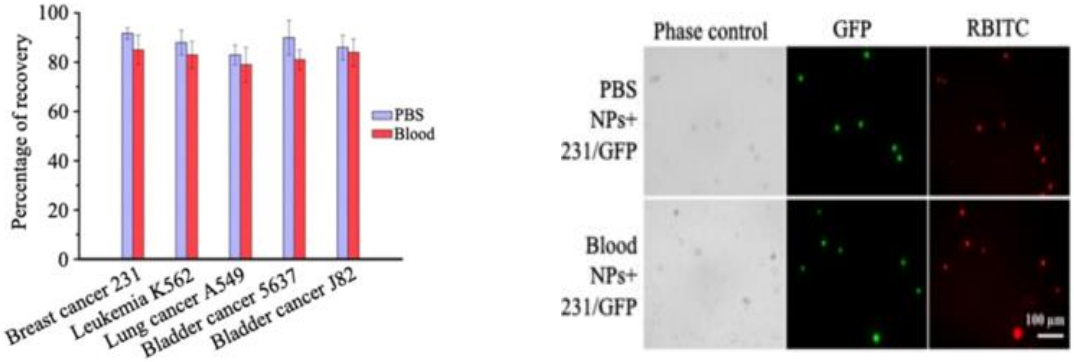

d) e)

Figure 1. Advanced nanomaterial CTC detection system utilizing the negative surface charge property of cancer cells.

(a) Schematic representation of the charge-mediated CTC isolation procedure. (1) acquisition of peripheral blood; (2) plasma depletion via centrifugation followed by resuspension of cellular components; (3) introduction of nanoprobes and incubation; (4) magnetic collection under an external magnetic field; (5) multiple washes to clear unbound material; (6) harvesting of enriched cells; (7) characterization of isolated cell populations. (b) Recovery rates observed when 20–250 cells were spiked into PBS or blood. (c) Recovery rates when 0–30 × 10^5 cells were spiked into PBS or blood. (d) Enrichment efficiency for multiple cancer cell types from both PBS and simulated blood environments. (e) Representative fluorescence micrographs of recovered cells from buffer and simulated blood matrices. MDA-MB-231 breast cancer cells stably express green fluorescent protein (GFP), allowing straightforward confirmation of spiked tumor cells. The positively charged nanomagnetic particles (NPs+) were conjugated with Rhodamin B Isothiocyanate (RBITC). Scale bar, 100 μm.

As depicted in **Figure 1b**, more than 95% of spiked control cells were retrieved from PBS and over 85% from blood at concentrations below 250 cells per mL. Recovery efficiency dropped to roughly 70% at a high concentration of three million cells per mL **(Figure 1c)**, revealing that the platform reaches capacity around one million target cells per mL in either medium. Comparable recovery levels were observed across diverse cancer cell lines tested in both PBS and blood **(Figure 1d)**. **Figure 1e** presents characteristic images under fluorescence microscopy of isolated MDA-MB-231 cells from PBS and blood, displaying the corresponding fluorescent signals. Additional validation was performed using a murine tumor model, which demonstrated successful CTC detection in peripheral blood from mice bearing S180 sarcoma or 4T1 breast tumors. In conclusion, these control experiments establish that the NPs effectively recover tumor cells from blood samples.

Using biomarkers to evaluate the captured cancer cells

To further characterize the enriched population, immunofluorescence staining was conducted on the isolated cells. After recovering A549 lung cancer cells from whole blood via the established procedure, nuclei were counterstained with DAPI. CD45 served to identify leukocytes, while CK19 and EpCAM were applied as epithelial markers. As presented in **Figure 2**, CD45 labeling was confined to leukocytes, in contrast to CK19 and EpCAM, which specifically highlighted the A549 tumor cells. These observations demonstrate the concurrent presence of leukocytes and epithelial-derived malignant cells following enrichment, thereby confirming the reliability and selectivity of the nanoprobe system.

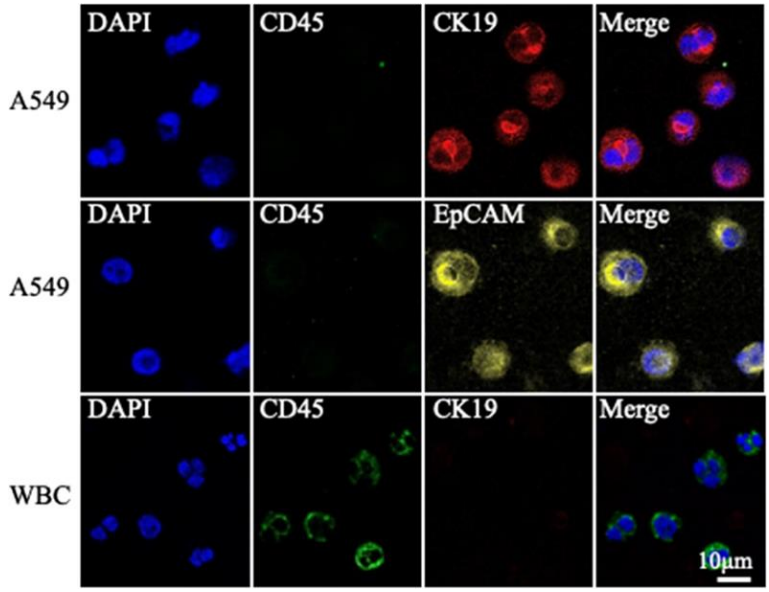

Figure 2. Representative immunofluorescence micrographs used for phenotypic identification of cells obtained from simulated clinical blood samples.

A549 lung cancer cells were spiked into whole blood to assess the new nanotechnology platform. White blood cells (WBC) acted as reference controls. Recovered cancer cells were predominantly CD45-/CK19+ and CD45-/EpCAM+, whereas leukocytes displayed mainly CD45+/CK19- and CD45+/EpCAM- profiles. DAPI (4′,6-diamidino-2-phenylindole) was employed as a nuclear stain; CD45 denotes leukocyte common antigen; CK19 indicates cytokeratin 19; EpCAM refers to epithelial cell adhesion molecule. Scale bar, 10 μm.

Capture of leukemia blasts from blood samples of leukemia patients

A subset of each clinical blood specimen, collected from individuals diagnosed with leukemia in a clinical pathology laboratory, was processed using the current technique. Samples from healthy volunteers were examined in parallel. The entire experimental workflow was performed in a double-blind manner until cell enumeration was completed. Consequently, no tumor cells were recovered from the blood of healthy donors using either positively or negatively charged NPs **(Figures 3a and 3b)**. Likewise, negative NPs yielded no cells from either healthy donors or leukemia patients **(Figures 3a, 3c, 3e and 3g)**. In contrast, positive NPs successfully isolated substantial quantities of cells from leukemia patients **(Figures 3d, 3f, and 3h)**. Cytological examination revealed that the vast majority of these captured cells displayed morphological features consistent with leukemia blast cells. These observations demonstrate that the positively charged NPs effectively enriched leukemic blasts from patient blood.

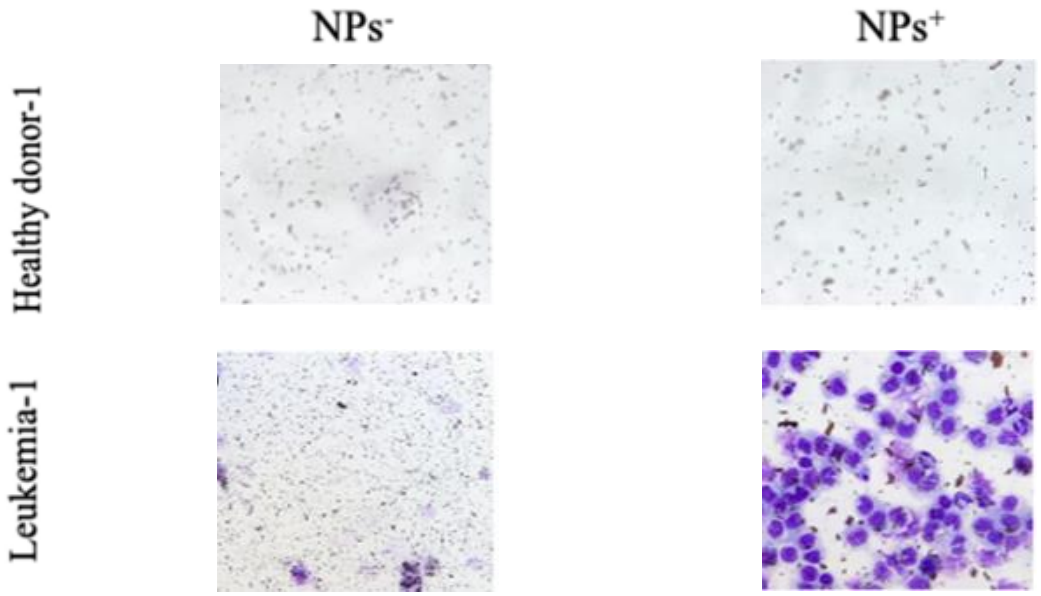

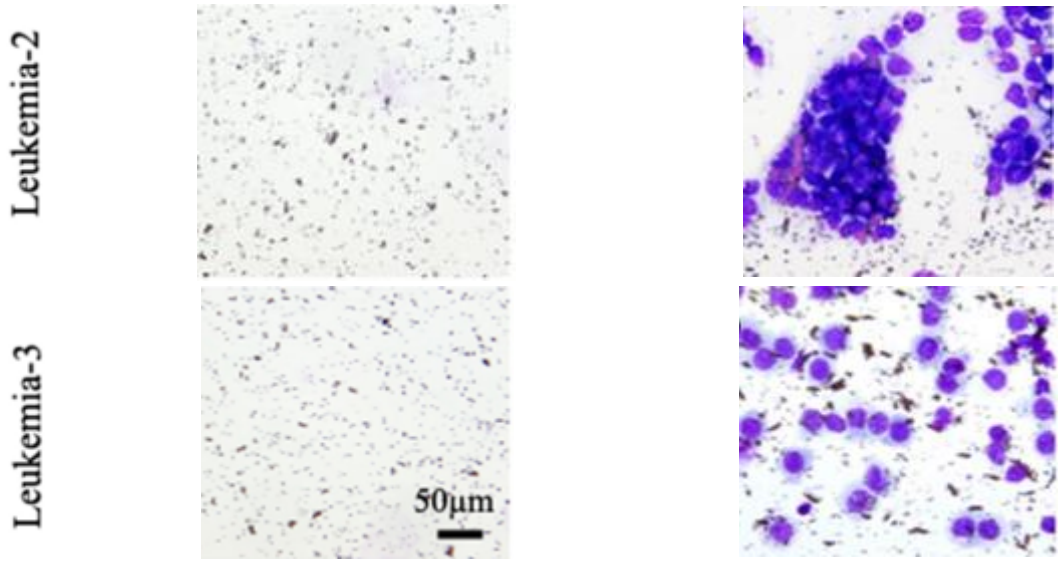

Figure 3. Diff-Quik staining of cells recovered using negatively and positively charged NPs from blood specimens of leukemia patients.
(a, b) Images of cells obtained from healthy donor blood samples. (c–h) Images of cells obtained from blood samples of three different leukemia patients. Scale bar is 50 μm.

Nevertheless, when compared with the blast counts and blast percentages among total leukocytes reported by the clinical pathology laboratory, the number of cells recovered from leukemia samples represented only a modest fraction of the total blasts, varying between 1.4% and 43.6%. Drawing on data from earlier control experiments, two main explanations may account for these lower recovery percentages. Unlike the pathology laboratory, which determines leukemia blast numbers through direct microscopic counting of all white blood cells and blasts after staining, the present method relies on a fixed quantity of NPs for enrichment. Thus, the first explanation is that extremely high leukemia cell burdens in certain samples may have surpassed the binding capacity of the NPs. Control experiments previously showed a sharp decline in recovery efficiency once cell concentrations exceeded one million per mL of blood, a threshold greatly surpassed by many of the clinical leukemia samples. The second possibility is that not all viable leukemia cells circulating in patient blood are metabolically active, unlike the control cells cultured under proliferative (log-phase) conditions. Such non-proliferating cells are considered dormant. In the dormant state, leukemia cells cease to produce significant levels of lactic acid through intense glycolysis and consequently lose their negative surface charge. Together, these two factors likely explain the discrepancy between the cells isolated by the nanomaterial platform and the total blast counts determined by conventional pathological evaluation.

Capturing cells from the blood samples of solid cancer patients

The performance of this nanomaterial platform in identifying CTCs among patients with solid malignancies was subsequently examined. Peripheral blood specimens were typically acquired from individuals shortly after confirmation of metastatic spread and prior to any therapeutic intervention. Control samples originated from healthy volunteers and from patients with localized bladder carcinoma in situ lacking evidence of metastasis. **Figure 4** presents characteristic micrographs of enriched cells derived from blood of patients diagnosed with diverse advanced cancers. Quantitative summaries of mean and median CTC counts per cancer type, along with positive detection frequencies, are provided in **Figure 5 and Table 1**. Notably, the yield of captured cells was substantially greater in samples from patients exhibiting distant metastases relative to those from healthy donors and individuals with non-metastatic bladder disease. This pattern aligns with the established association between circulating cancer cells and aggressive, metastatic tumor behavior.

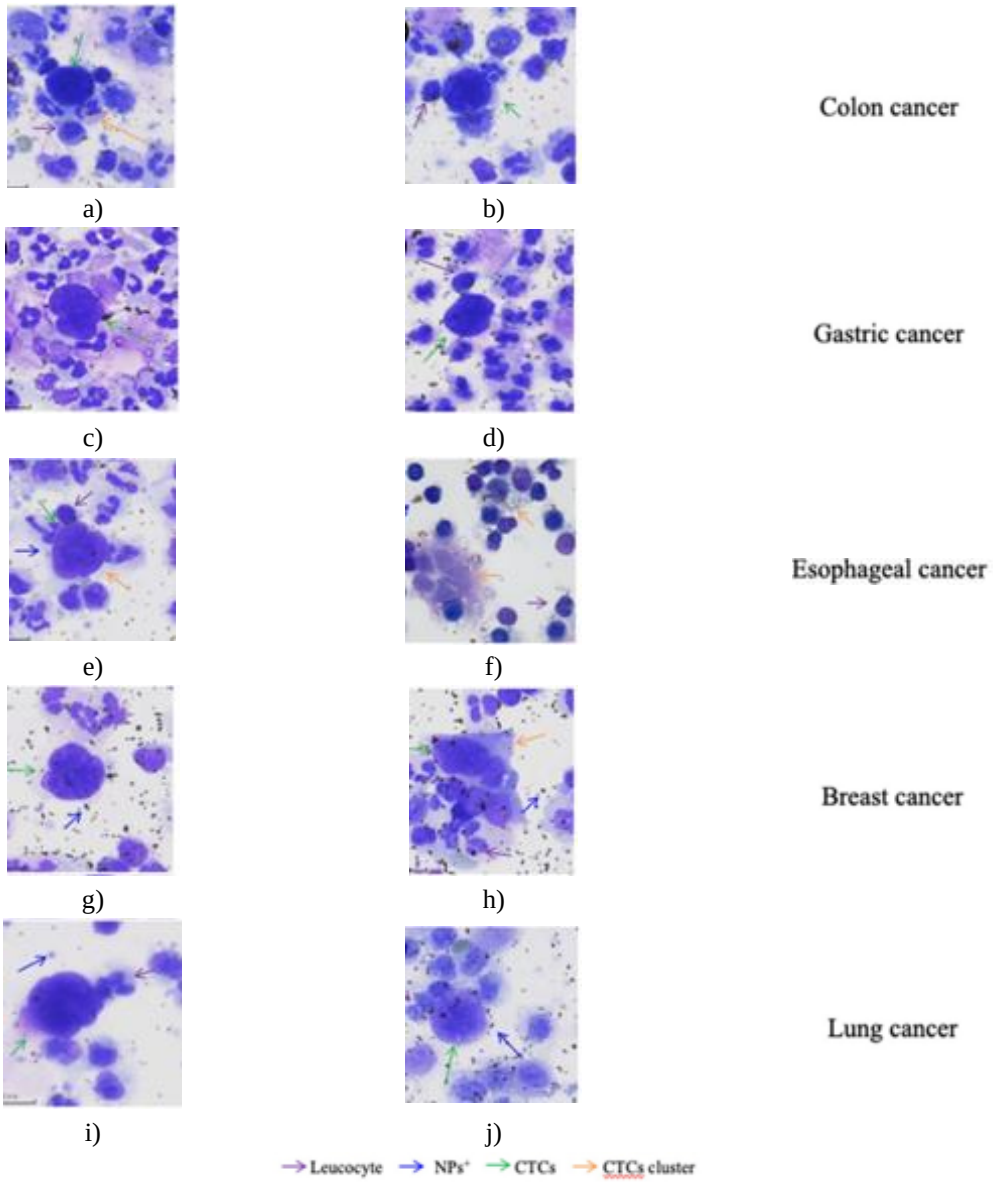

Figure 4. Representative morphology of cells isolated using positively charged nanomagnetic particles (NPs+) from patient blood specimens.
(a, b) CTCs obtained from two colon cancer cases, one of which contained a CTC cluster (yellow arrow). (c, d) CTCs obtained from two gastric cancer cases. (e, f) CTCs obtained from two esophageal cancer cases, both displaying CTC clusters. (g, h) CTCs obtained from two breast cancer cases, with a CTC cluster visible in one sample. (i, j) Numerous primary tumor cells recovered from two lung cancer specimens via NPs+. Scale bar, 20 μm.

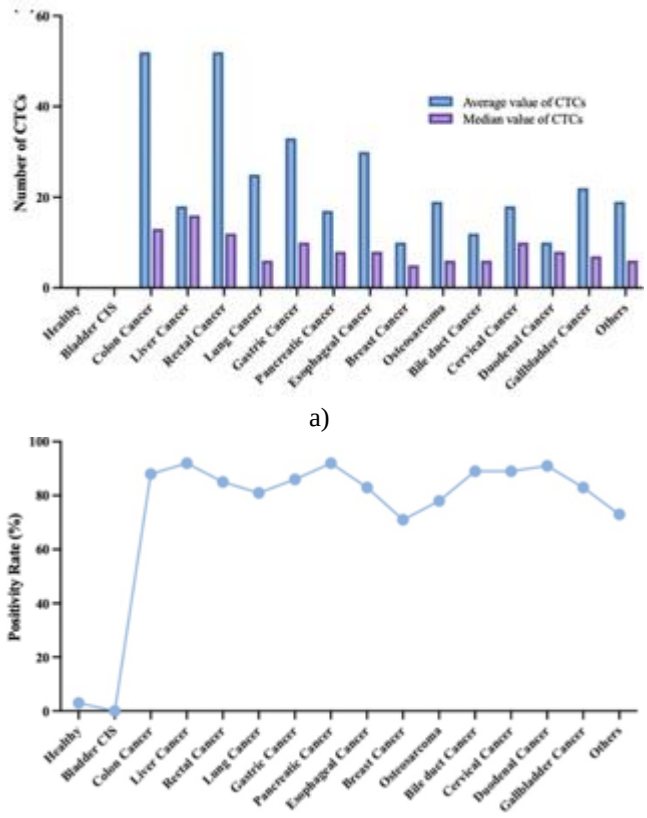

Figure 5. Enumeration of CTCs isolated by NPs+ from healthy individuals and patients with solid tumors.

No CTCs were identified in blood from healthy donors or patients with early-stage bladder carcinoma in situ (CIS). Advanced solid tumor samples included 386 colon cancer cases, 321 liver cancer cases, 265 rectal cancer cases, 295 lung cancer cases, 153 gastric cancer cases, 117 pancreatic cancer cases, 127 esophageal cancer cases, 138 breast cancer cases, 79 osteosarcoma cases, 46 bile duct cancer cases, 19 cervical cancer cases, 23 duodenal cancer cases, 18 gallbladder cancer cases, and 314 cases involving other malignancies, all sourced from Quanzhou First Hospital in Fujian and Tongji University Oriental Hospital in Shanghai. CTC quantification was performed per mL of blood following staining and microscopic assessment. (a) Mean and median CTC numbers for each cancer type. (b) Positive detection rates for each cancer type.

Table 1. Quantification of CTCs captured by NPs+ from healthy donors and solid cancer patients.

Disease group	CTC-positive (n)	CTC-negative (n)	Positivity rate (%)	Mean CTC count	Median CTC count
Healthy controls	16	536	2.9	0	0
Bladder CIS	0	6	0	0	0
Colon cancer	339	47	87.8	52	13
Liver cancer	296	25	92.2	18	16
Rectal cancer	225	40	84.9	52	12
Lung cancer	240	55	81.4	25	6
Gastric cancer	132	21	86.3	33	10
Pancreatic cancer	108	9	92.3	17	8
Esophageal cancer	105	22	82.7	30	8
Breast cancer	98	40	71.0	10	5
Osteosarcoma	62	17	78.5	19	6
Bile duct cancer	41	5	89.1	12	6
Cervical cancer	17	2	89.5	18	10
Duodenal cancer	21	2	91.3	10	8

Gallbladder cancer	15	3	83.3	22	7
Other cancers	228	86	72.6	19	6

Additional assessments explored CTC recovery in relation to pathologic TNM staging. The analyses revealed superior performance of the platform in stage III and IV disease, manifested by both increased detection frequencies and higher cell yields **(Figure 6 and Table 2)**. Such outcomes underscore the potential clinical role of this CTC detection strategy in aiding pathologic disease staging.

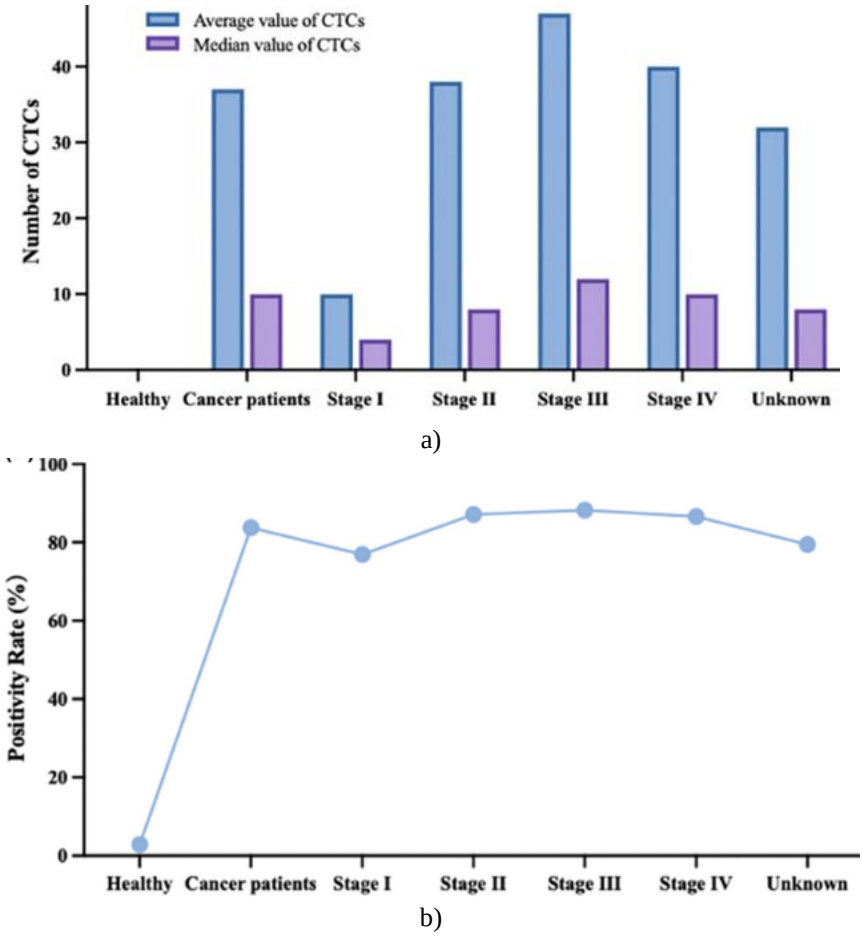

Figure 6. Statistical assessment of CTCs recovered by NPs+ across cancer patient cohorts.

Blood samples were obtained from 2301 individuals diagnosed with various solid tumors (including lung, colon, esophageal, rectal, and other cancers) at Quanzhou First Hospital in Fujian and Tongji University Oriental Hospital in Shanghai, along with 552 healthy controls. The cohort comprised 39 stage I patients, 140 stage II patients, 255 stage III patients, 933 stage IV patients, and 934 patients with undetermined or unknown stages. All cases were stratified according to pathologic TNM classification. CTCs were evaluated per mL of blood. (a) Mean and median CTC counts by disease stage. (b) Positive detection rates by disease stage.

Table 2. Statistical analyses of CTCs captured by NPs+ from cancer patient samples.

Group	CTC-positive (n)	CTC-negative (n)	Detection rate (%)	Mean CTC count	Median CTC count
Healthy controls	16	536	2.9	0	0
Cancer patients (overall)	1927	374	83.75	37	10
Stage I	30	9	76.92	10	4
Stage II	122	18	87.14	38	8
Stage III	225	30	88.24	47	12
Stage IV	808	125	86.60	40	10
Stage unknown	742	192	79.44	32	8

Further immunophenotypic analysis of the enriched cells was conducted using fluorescent labeling for nuclear material (DAPI), leukocyte marker (CD45), and epithelial markers (CK19 and EpCAM) **(Figure 7)**. Captured cells consistently lacked CD45 expression, confirming their non-leukocyte identity. While epithelial markers CK19 and EpCAM were detectable, they appeared in only a limited proportion (ranging from 10% to 50%) of the total isolated cell population. This partial and heterogeneous expression is consistent with the occurrence of epithelial-mesenchymal transition (EMT) in many disseminated cancer cells, which frequently results in reduced or absent classical epithelial surface proteins.

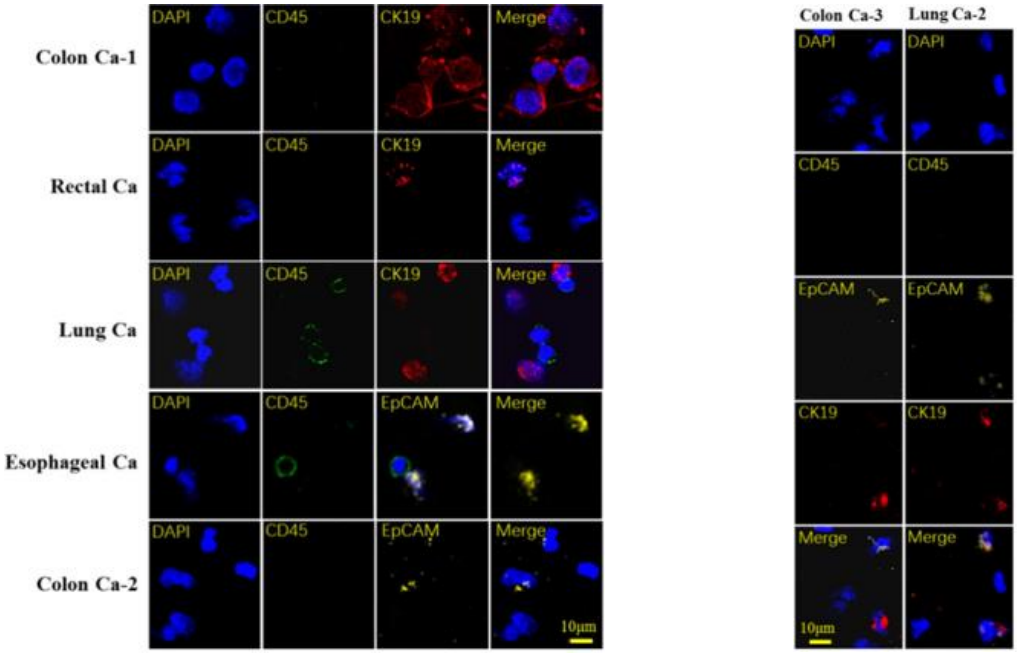

Figure 7. Representative immunofluorescence images for characterization of cells enriched by NPs+ from clinical blood specimens.

(a) Cells displaying DAPI+/CD45-/CK19+ or DAPI+/CD45-/EpCAM+ phenotypes were designated as CTCs, whereas DAPI+/CD45+/CK19- or DAPI+/CD45+/EpCAM- cells were classified as white blood cells (WBCs). A CTC cluster showing DAPI+/CD45-/CK19+ staining was observed in one colon cancer sample. In several rectal and colon cancer cases, roughly half the cells expressed CK19 or EpCAM while the remaining cells lacked these markers along with CD45. Samples from lung and esophageal cancers similarly contained CD45-/CK19+ populations. (b) In colon cancer case 2 and lung cancer case 2, variable expression of CK19 and EpCAM was noted, with some cells negative for both markers, illustrating surface protein heterogeneity among CTCs. DAPI, 4′,6-diamidino-2-phenylindole, is a nuclear dye; CD45, leukocyte common antigen; CK19, cytokeratin 19; EpCAM, epithelial cell adhesion molecule. Scale bar, 10 μm.

Extending our 2016 findings on the negative surface charge exhibited by cultured cancer cells [26], the central aim of the present investigation was to assess whether a nanotechnology approach directed at this biophysical property could successfully isolate CTCs from clinical blood specimens of cancer patients. The study examined more than 2000 clinical cases spanning a broad spectrum of malignancies, including leukemia. The outcomes demonstrate that the proposed nanotechnology platform achieves efficient and reliable CTC capture from blood samples, attaining an overall sensitivity of 83.75% and specificity of 97.10%. Recovered CTC counts per mL of blood from patients with solid tumors or leukemia ranged from several hundred to tens of thousands. These yields substantially exceed those typically obtained with most existing methods, which generally recover only up to a few dozen cells from 7.5 mL of blood. Moreover, the platform proved especially effective at isolating higher numbers of CTCs from patients with advanced (stages III–IV) disease. Taken together, these data highlight the promising clinical value of the developed nanotechnology.

Existing CTC enrichment strategies primarily rely on epithelial surface markers such as EpCAM or on intrinsic physical attributes like cell size. However, the intrinsic heterogeneity of CTCs limits the performance of these conventional approaches in terms of both efficiency and specificity. In contrast, the current technology exploits

the unique surface charge properties that distinguish cancer cells from normal blood cells. Earlier studies have established that cancer cells possess a negative surface charge resulting from increased lactate production associated with heightened glycolytic activity [28]. Elevated glucose consumption and lactate secretion represent hallmark metabolic features of active cancer cells. The combination of high glucose uptake, substantial lactate release, and consequent negative surface charge appears to be among the few phenotypic traits common to most, if not all, metabolically active cancer cells, including leukemia blasts [29]. By comparison, normal cells predominantly depend on oxidative phosphorylation, producing H_2O and CO_2 instead of lactate, and therefore lack a significant negative surface charge [26, 30]. This fundamental difference enables the selective separation of malignant cells from normal blood elements based on surface charge, without dependence on specific cell surface proteins. As a result, the present nanotechnology provides a clear advantage over marker-dependent methods, delivering markedly improved sensitivity for CTC detection.

Furthermore, this study represents the first instance in which cancer cells isolated from actual patient blood samples were identified and quantified using standard cytological staining protocols (Diff-Quik) routinely employed in pathology laboratories. The morphology of the captured CTCs closely matched that of recognized malignant cells and typically displayed the following features: (1) they were distinct from any normal blood cell types; (2) they possessed markedly enlarged nucleoli (≥10 μm); (3) they exhibited large overall cell size (≥20 μm) with thin, sparsely distributed cytoplasm; (4) they frequently formed clusters with other captured cells or normal blood elements; (5) their nuclei often showed irregular contours rather than smooth, rounded shapes; and (6) their cytoplasm stained lightly while nucleoli appeared darker relative to normal cells [31-33]. On the basis of these morphological criteria, the isolated cells were readily distinguishable from normal blood constituents and conformed to the cytological appearance of known cancer cells. Direct cytomorphological assessment continues to serve as the primary standard for initial cancer diagnosis in clinical practice. In contrast, many prior CTC detection approaches have depended on immunofluorescence targeting specific tumor markers, which are more suitable for secondary analyses aimed at subtype or origin determination. Accordingly, we contend that direct morphological evaluation using established clinical cytological standards offers greater reliability for identifying cells associated with metastatic disease than methods relying predominantly on indirect marker-based detection.

Owing to its affordability and minimally invasive character, the described technique is expected to find wide application in clinical diagnostics and population screening. Additionally, the efficient recovery of large numbers of leukemia cells underscores the platform's ability to detect heightened glycolytic activity in blood, suggesting strong potential within hematologic oncology. Application of this approach to solid tissues or organs has so far been limited by uncertainty regarding whether different cell populations within solid tissues display comparable surface charge characteristics. Moreover, evaluating surface charge in solid tissue sections is technically challenging, as procedures such as cryopreservation, fixation, and staining disrupt cell viability and metabolic function [34].

Conclusion

In summary, the present study confirms that a negative surface charge represents a shared feature of all glycolytically active cancer cells. The newly developed nanotechnology effectively targets this property, allowing selective isolation of malignant cells, including leukemia blasts, from normal blood components. Evaluation across nearly 2000 clinical cases demonstrated that the method recovers CTCs at levels orders of magnitude higher than previously reported technologies. The isolated cancer cells remain viable and suitable for multiple downstream applications, including cell culture, genomic sequencing, drug sensitivity testing, and single-cell profiling [35-37]. Given its high efficiency and non-invasive profile, this technology holds considerable promise for widespread use in clinical assessment and broad-scale cancer screening.

Acknowledgments: None

Conflict of Interest: None

Financial Support: None

Ethics Statement: None

References

1. Moss TJ, Sanders DG, Lasky LC, Bostrom B. Contamination of peripheral blood progenitor cell products with malignant cells. Blood. 1990;76(9):1879-85.
2. Cortés-Hernández LE, Eslami SZ, Pantel K, Alix-Panabières C. Molecular and functional characterization of circulating tumor cells: from basic research to clinical application. Clin Chem. 2020;66(1):97-106.
3. Massagué J, Obenauf AC. Metastatic colonization by circulating tumour cells. Nature. 2016;529(7586):298-306.
4. Kantamneni H, Zevon M, Donzanti MJ, Zhao X, Sheng Y, Barkund SR, et al. Surveillance nanotechnology for monitoring the metastatic potential of circulating tumor cells. Nat Biomed Eng. 2017;1(12):993-1005.
5. Mazzone M, Bergers G. Regulation of the angiogenic switch in cancer. Annu Rev Physiol. 2019;81:535-60.
6. Li XY, Dong M, Zang XY, Li MY, Zhou JY, Ma JJ, et al. The emerging role of circulating tumor cells in cancer diagnosis and treatment. Am J Transl Res. 2020;12(2):332-45.
7. Schuster E, Taftaf R, Reduzzi C, Albert MK, Romero-Calvo I, Liu H. The role of circulating tumor cells in the metastatic cascade. Trends Cancer. 2021;7(11):1020-33.
8. Valastyan S, Weinberg RA. Tumor metastasis: molecular insights and evolving paradigms. Cell. 2011;147(2):275-92.
9. Lambert AW, Pattabiraman DR, Weinberg RA. Emerging biological principles of metastasis. Cell. 2017;168(4):670-91.
10. Liu WR, Zhang B, Chen C, Li Y, Ye X, Tang DJ, et al. Circulating tumor cells (CTCs) in lung cancer: current status and future perspectives. Thorac Cancer. 2020;11(11):3234-45.
11. Lawrence R, Watters M, Davies CR, Pantel K, Lu YJ. Liquid biopsy in cancer: biology and clinical implications. Nat Rev Clin Oncol. 2023;20(7):487-505.
12. Arber DA, Orazi A, Hasserjian R, Thiele J, Borowitz MJ, Le Beau MM, et al. The 2016 revision to the World Health Organization classification of myeloid neoplasms and acute leukemia. Blood. 2016;127(20):2391-405.
13. Jackson JM, Taylor JB, Witek MA, Hunsucker SA, Waugh JP, Fedoriw Y, et al. Development of a microfluidic device for the isolation of circulating tumor cells. Analyst. 2016;141(2):640-8.
14. Gabriel MT, Calleja LR, Chalopin A, Ory B, Heymann D. Circulating tumor cells in bone metastasis: clinical relevance and molecular mechanisms. Clin Chem. 2016;62(4):571-81.
15. Andree KC, van Dalum G, Terstappen LW. Challenges in the enumeration and characterization of circulating tumor cells. Mol Oncol. 2016;10(3):395-407.
16. Nagrath S, Sequist LV, Maheswaran S, Bell DW, Irimia D, Ulkus L, et al. Isolation of rare circulating tumour cells in cancer patients by microchip technology. Nature. 2007;450(7173):1235-9.
17. Li Y, Lu Q, Liu H, Wang J, Zhang P, Liang H, et al. Detection of circulating tumor cells using a novel integrated microfluidic device. Adv Mater. 2015;27(43):6848-54.
18. Hyun KA, Lee TY, Jung HI. Microfluidic platform for the isolation and detection of circulating tumor cells. Anal Chem. 2013;85(9):4439-45.
19. Desitter I, Guerrouahen BS, Benali-Furet N, Wechsler J, Jänne PA, Kuang Y, et al. A new device for the isolation of circulating tumor cells from blood samples. Anticancer Res. 2011;31(2):427-41.
20. Wang L, Asghar W, Demirci U, Wan Y. Nanostructured substrates for isolation of circulating tumor cells. Nano Today. 2013;8(4):347-60.
21. Pantel K, Alix-Panabières C. Liquid biopsy and minimal residual disease - latest advances and implications for cure. Nat Rev Clin Oncol. 2019;16(7):409-24.
22. Gorges TM, Tinhofer I, Drosch M, Röse L, Zollner TM, Krahn T, et al. Circulating tumour cells escape from EpCAM-based detection due to epithelial-to-mesenchymal transition. BMC Cancer. 2012;12:178.
23. Zheng X, Carstens JL, Kim J, Scheible M, Kaye J, Sugimoto H, et al. Epithelial-to-mesenchymal transition is dispensable for metastasis but induces chemoresistance in pancreatic cancer. Nature. 2015;527(7579):525-30.
24. Ju S, Chen C, Zhang J, Xu L, Zhang X, Li Z, et al. Circulating tumor cells and their clinical applications in cancer. Biomark Res. 2022;10(1):58.
25. Hong B, Zu Y. Detecting circulating tumor cells: current challenges and new trends. Theranostics. 2013;3(6):377-94.

26. Chen B, Le W, Wang Y, Li Z, Wang D, Ren L, et al. Targeting negative surface charges of cancer cells by multifunctional nanoprobes. Theranostics. 2016;6(11):1887-98.
27. Hanahan D, Weinberg RA. Hallmarks of cancer: the next generation. Cell. 2011;144(5):646-74.
28. Faubert B, Li KY, Cai L, Hensley CT, Kim J, Zacharias LG, et al. Lactate metabolism in human lung tumors. Cell. 2017;171(2):358-71.
29. Sasca D, Szybinski J, Schüler A, Shah V, Heidelberger J, Haehnel PS, et al. Fatty acid synthesis is required for survival of AML cells. Blood. 2019;133(21):2305-17.
30. Le W, Chen B, Cui Z, Liu Z, Shi D. Detecting circulating tumor cells with nanotechnology. Biophys Rep. 2019;5(1):10-6.
31. Harada S, Agosto-Arroyo E, Levesque JA, Alston E, Janowski KM, Coshatt GM, et al. Cytologic features of circulating tumor cells in breast cancer patients. Cancer Cytopathol. 2015;123(8):480-8.
32. Baba AI, Câtoi C. Comparative Oncology. Bucharest (RO): The Publishing House of the Romanian Academy; 2007.
33. Singh I, Lele TP. Cell-cell interactions in the tumor microenvironment. Results Probl Cell Differ. 2022;70:443-68.
34. Hashimoto K, Nishimura S, Ito T, Oka N, Akagi M. Circulating tumor cells in gastrointestinal cancers. Ann Med Surg. 2021;68:102581.
35. Mohamed BM, Ward MP, Bates M, Spillane CD, Kelly T, Martin C, et al. Heterogeneity of circulating tumor cells in breast cancer. Sci Rep. 2023;13(1):3704.
36. Xu J, Liao K, Yang X, Wu C, Wu W. Circulating tumor cells: biology and clinical significance in cancers. Mol Cancer. 2021;20(1):104.
37. Negishi R, Yamakawa H, Kobayashi T, Horikawa M, Shimoyama T, Koizumi F, et al. Development of a novel method for the detection of circulating tumor cells. Commun Biol. 2022;5(1):20.